DNA Bases Ring-Expanded with Cyclopentadiene Free Radical: A theoretical investigation on Building Blocks with Diradical Characteristics

Peiwen Zhao, Yuxiang Bu*

School of Chemistry and Chemical Engineering, Shandong University, Jinan, 250100, People's Republic of China

Corresponding Authors: byx@sdu.edu.cn

Electronic Supplementary Materials

1. Tables

Table S1. The Bond Energies and Bond Lengths of Trans-r-bases. For Comparison, Data of the Natural Bases are Given

Energy(a.u.)	**rA**		**rG**		**rC**		**rT**	
	-582.34		-657.621		-509.96		-529.86	
Bond Length (Å)	C_1-C_2	1.427 1.397	C_1-C_2	1.432 1.393	C_1-C_2	1.430 1.356	C_1-C_2	1.425 1.349
	C_1-C_5	1.474	C_1-N_5	1.463	C_1-C_4	1.435 1.440	C_1-N_5	1.356 1.349
	C_1-N_{14}	1.33 1.366	C_1-N_{15}	1.347 1.356	C_1-C_{12}	1.395	C_1-C_{11}	1.438
	C_2-C_3	1.394 1.409	C_2-C_3	1.423 1.438	C_2-N_{10}	1.340	C_2-C_3	1.445 1.467
	C_2-C_7	1.436	C_2-C_7	1.422	C_2-C_{13}	1.438	C_2-C_{10}	1.391 1.500
	C_3-N_{10}	1.356 1.353	C_3-O_{10}	1.218 1.213	C_3-N_9	1.363 1.369	C_3-O_7	1.214 1.217
	C_3-N_{13}	1.357 1.342	C_3-N_{14}	1.447 1.439	C_3-N_{10}	1.445 1.428	C_3-N_9	1.424 1.407
	C_4-N_{13}	1.349 1.341	C_4-N_{14}	1.358 1.370	C_3-O_{11}	1.217 1.216	C_4-N_5	1.406 1.388
	C_4-N_{14}	1.326 1.334	C_4-N_{15}	1.322 1.308	C_4-N_6	1.355 1.361	C_4-N_9	1.380 1.384
	C_5-N_6	1.382	C_4-N_{11}	1.366 1.375	C_4-N_9	1.321 1.317	C_4-O_8	1.212 1.214

	C_6-N_7	1.428	C_5-C_6	1.372	C_{12}-C_{14}	1.444	C_{10}-C_{12}	1.449
	C_6-N_{16}	1.386	C_6-C_7	1.446	C_{13}-C_{14}	1.378	C_{11}-C_{12}	1.377
	C_7-N_{15}	1.357 1.384	C_6-N_{16}	1.383 1.369	N_{10}-H_5	1.012	N_5-H_{13}	1.011 1.009
	N_{10}-H_{11}	1.007 1.006	C_7-N_{17}	1.36 1.380	N_6-H_7	1.005 1.005	N_9-H_6	1.012 1.013
	N_{15}-H_{17}	1.329 1.308	N_{16}-C_{18}	1.382 1.385				
	N_{16}-C_{17}	1.376 1.380	N_{17}-C_{18}	1.322 1.304				
	N_{16}-H_{18}	1.007 1.008	N_{11}-H_{11}	1.01 1.01				
			N_{11}-H_{12}	1.01 1.01				
			N_{16}-H_{20}	1.01 1.01				

Table S2. Binding Energies (kcal /mol^{-1}) of Natural Bases and Trans-r-bases

BP	BE	BP	BE
G-C	-25.72	rG-C	-26.82
		G-rC	-25.06
		rG-rC	-26.10
A-T	-12.67	rA-T	-12.00
		A-rT	-12.75
		rA-rT	-12.40

Table S3. (AIP, VIP）and (AEA, VEA) of the Natural Bases and Trans-r-bases (eV)

Bases	AIP	VIP	AEA	VEA
T	8.81	9.05	0.01	-0.24
A	7.55	8.01	-0.16	-0.31
G	8.11	8.31	-0.33	-0.45
C	8.63	8.75	-0.11	-0.26
rT	7.88	8.24	2.58	2.28
rG	6.66	7.79	2.05	2.07
rA	6.97	7.24	2.06	1.61
rC	7.45	8.52	2.37	2.48

Table S4. The Frontier Orbital Energies and Corresponding Energy Gaps of Trans-r-bases

Bases	HOMO	LUMO	Gaps	r-Bases	SOMO	LUMO	Gaps
G	-6.12	-0.87	5.25	rG	-5.26	-0.82	4.44
A	-6.34	-0.99	5.35	rA	-5.44	-0.74	4.70
C	-6.67	-1.28	5.39	rC	-5.87	-1.27	4.60
T	-6.99	-1.58	5.42	rT	-6.26	-1.25	5.01

Table S5. Frontier Orbitals Occupation Numbers of Open-Shell Singlet States，Magnetic Exchange Coupling Constants (J in cm^{-1}) of the Overlap-Stacking Trans-r-base Pairs. Four Different J Values Represent Situations in Trans-r-base Pairs (J), Rise Changes in Trans-r-base Pairs (J') and r-base Pairs (J^*)

Groups	BPs	Occupation Numbers		J Values(cm^{-1})		
		HOMO	LUMO	J	J'	J^*
3′-rPu/ 5′-rPu	rG-C/rG-C	1.167	0.901	-1449.6	-24.7	16.4
	rG-C/rA-T	1.102	0.856	-1670.0	-55.2	32.1
	rA-T/rA-T	1.270	0.730	-284.7	-68.2	28.4
	rA-T/rG-C	1.077	0.923	-355.9	-26.0	108.3
3′-rPy/ 5′-rPy	G-rC/G-rC	1.948	0.828	-126.0	-103.8	-226.0
	G-rC/A-rT	1.950	0.769	290.8	-36.0	-184.8
	A-rT/A-rT	1.234	0.768	-352.4	-195.8	-194.4
	A-rT/G-rC	1.102	0.900	-76.2	-39.4	-326.4
3′-rPu/ 5′-rPy	rG-C/rC-G	1.057	0.943	0.13	177.6	-8.3
	rG-C/rT-A	1.044	0.955	-80.9	206.8	-9.9
	rA-T/rT-A	1.265	0.735	-164.7	-73.6	-16.0
	rA-T/rC-G	1.212	0.788	474.7	-233.0	-8.2
3′-rPy/ 5′-rPu	rC-G/rG-C	1.099	0.901	-175.9	-291.1	-1075.1
	rC-G/rA-T	1.180	0.823	-107.2	2.05	-425.9
	rT-A/rA-T	1.157	0.843	-155.9	-917.9	-359.8
	rT-A/rG-C	1.103	0.897	-51.9	-67.1	-695.9

Table S6. Frontier Orbitals Occupation Numbers of Open-Shell Singlet States，Magnetic Exchange Coupling Constants (J in cm^{-1}) of the Cross-Stacking Diradical Base Pairs. Four Different J Values Represent Situations in Trans-r-base Pairs (J), Rise Changes in Trans-r-base Pairs (J'') and r-base Pairs (J^*)

Groups	BPs	Occupation Numbers		J Values		
		HOMO	LUMO	J	J'	J^*
3'-rPu 3'-rPu	rG-C/C-rG	1.001	0.999	12.2	-294.8	-5.2
	rG-C/T-rA	1.000	1.000	1.2	31.7	-11.1
	rA-T/T-rA	1.020	0.981	0.0	229.9	-24.3
5'-rPu 5'-rPu	C-rG/rG-C	1.012	0.988	-11.5	-326.4	-0.2
	T-rA/rG-C	0.999	1.000	-2.0	-28.7	0.0
	T-rA/rA-T	1.000	0.999	0.0	-71.3	0.0
3'-rPy 3'-rPy	rC-G/G-rC	0.998	1.004	-0.8	-494.9	0.0
	rC-G/A-rT	1.000	1.002	-0.1	96.7	0.0
	rT-A/A-rT	1.000	0.999	0.0	0.0	0.0
5'-rPy 5'-rPy	G-rC/rC-G	1.000	1.002	0.2	-40.0	0.0
	G-rC/rT-A	1.000	1.000	0.0	-24.4	0.0
	A-rT/rT-A	1.001	1.000	0.0	177.6	0.0
3'-rPu/ 3'-rPy	rG-C/G-rC	1.013	0.987	-103.8	-92.4	-0.4
	rG-C/A-rT	1.013	0.987	-158.5	50.3	-3.6
	rA-T/A-rT	1.000	1.000	0.0	0.0	-1.7
	rA-T/G-rC	1.003	0.998	0.4	-52.2	-0.4
5'-rPy/ 5'-rPu	G-rC/rG-C	1.000	0.999	-385.5	-127.3	-0.1
	G-rC/rA-T	1.029	0.972	-107.2	20.1	0.0
	A-rT/rA-T	1.000	1.000	0.0	52.9	0.0
	A-rT/rG-C	1.010	0.991	-169.3	-66.1	0.0

Table S7. Energies (in au, the Energies of the Closed-Shell States are Used as Benchmark) of the Tetra-Radical Two-layered Trans-r-base Pairs

Groups	BPs	Energies		
		E_{BS}	E_T	E_{CS}
Overlap	rG-rC/rG-rC	-2335.201	-2335.206	-2335.178
	rG-rC/rA-rT	-2279.804	-2279.810	-2279.788
	rA-rT/rA-rT	-2224.347	-2224.330	-2224.347
	rA-rT/rG-rC	-2279.794	-2279.810	-2279.794
3′-rPu/ 5′-rPy	rG-rC/rC-rG	-2335.198	-2335.193	-2335.198
	rG-rC/rT-rA	-2279.801	-2279.810	-2279.786
	rA-rT/rT-rA	-2224.338	-2224.336	-2224.334
3′-rPy/ 5′-rPu	rC-rG/rG-rC	-2335.143	-2335.142	-2335.135
	rC-rG/rA-rT	-2279.810	-2279.786	-2279.804
	rT-rA/rA-rT	-2224.404	-2224.401	-2224.394

Table S8. Frontier Orbitals Occupation Numbers of Open-Shell Singlet States of Tetra-Radical Two-layered Trans-r-base Pairs

Groups	BPs	HOMO-1	HOMO	LUMO	LUMO+1
Overlap	rG-rC/rG-rC	1.214	1.126	0.896	0.973
	rG-rC/rA-rT	1.140	1.434	0.860	0.566
	rA-rT/rA-rT	1.716	1.941	0.307	0.289
	rA-rT/rG-rC	1.175	1.245	0.825	0.754
3′-rPu/ 5′-rPy	rG-rC/rC-rG	1.362	1.142	0.858	0.638
	rG-rC/rT-rA	1.140	1.434	0.860	0.566
	rA-rT/rT-rA	1.452	1.324	0.679	0.548
3′-rPy/ 5′-rPu	rC-rG/rG-rC	1.151	1.341	0.959	0.721
	rC-rG/rA-rT	1.612	1.402	0.387	0.598
	rT-rA/rA-rT	1.463	1.321	0.679	0.537

Table S9. Frontier Orbitals Occupation Numbers of Open-Shell Singlet States of Tetra-Radical Two-layered Trans-r-base Pairs after Adjust the Rise

Groups	BPs	HOMO-1	HOMO	LUMO	LUMO+1
Overlap	rG-rC/rG-rC	1.189	1.097	0.903	0.878
	rG-rC/rA-rT	1.115	1.325	0.885	0.675
	rA-rT/rA-rT	1.970	1.318	0.437	0.682
	rA-rT/rG-rC	--	--	--	--
3′-rPu/ 5′-rPy	rG-rC/rC-rG	1.238	1.178	0.822	0.762
	rG-rC/rT-rA	0.995	1.000	1.000	1.005
	rA-rT/rT-rA	1.193	1.163	0.837	0.809
3′-rPy/ 5′-rPu	rC-rG/rG-rC	1.389	1.490	0.611	0.513
	rC-rG/rA-rT	0.979	1.574	1.021	0.427
	rT-rA/rA-rT	--	--	--	--

Table S10. Energy Order and Magnetic Exchange Coupling Constants (J in cm^{-1}) of Part Two-layered Trans-r-base Pairs. Open-Shell Singlet States calculated with UB3LYP/6-311++G** and UM062X/6-311++G**

BPs	UB3LYP/6-311++G**		UM062X/6-311++G**	
	Energy Order	J	Energy Order	J
rT-A/rA-T	$E_{BS}<E_T<E_{CS}$	-155.9	$E_{BS}<E_T<E_{CS}$	-190.8
rT-A/rG-C	$E_{BS}<E_T<E_{CS}$	-51.9	$E_{BS}<E_T<E_{CS}$	-91.9
rC-G/G-rC	$E_{BS}<E_T<E_{CS}$	-0.8	$E_{BS}<E_T<E_{CS}$	-0.4
rA-T/T-rA	$E_{BS}<E_T<E_{CS}$	0.0	$E_{BS}<E_T<E_{CS}$	-1.0
rC-G/rA-T	$E_{BS}<E_T<E_{CS}$	-107.2	$E_{BS}<E_T<E_{CS}$	-107.9
C-rG/rG-C	$E_{BS}<E_T<E_{CS}$	-11.5	$E_{BS}<E_T<E_{CS}$	-5.1
A-rT/G-rC	$E_{BS}<E_T<E_{CS}$	-76.2	$E_{BS}<E_T<E_{CS}$	-97.2
T-rA/rA-T	$E_T<E_{BS}<E_{CS}$	0.0	$E_{BS}\sim E_T<E_{CS}$	0.0

Table S11. Frontier Orbitals Occupation Numbers of Open-Shell Singlet States of part Two-layered Trans-r-base Pairs calculated with the CASSCF(10,10)/6-311+G* and CASSCF(8,8)/6-311+G* Methods

BPs	CASSCF(10,10)/6-311+G*				CASSCF(8,8)/6-31+G*			
	HOMO+1	HOMO	LUMO	LUMO-1	HOMO+1	HOMO	LUMO	LUMO-1
rT-A/rA-T	2.00	1.16	0.84	0	2.00	1.16	0.84	0
rT-A/rG-C	2.00	1.10	0.90	0	2.00	1.10	0.90	0
rC-G/G-rC	2.00	1.00	1.00	0	2.00	1.00	1.00	0
rA-T/T-rA	2.00	1.01	0.99	0	2.00	1.02	0.98	0
rC-G/rA-T	2.00	1.17	0.83	0	2.00	1.18	0.82	0
C-rG/rG-C	2.00	1.02	0.98	0	2.00	1.01	0.99	0
A-rT/G-rC	2.00	1.10	0.90	0	2.00	1.10	0.90	0
T-rA/rA-T	2.00	1.00	1.00	0	2.00	1.00	1.00	0

The Spin Densities Distributions of Expanded Trans-r-bases and Trans-r-base Pairs.

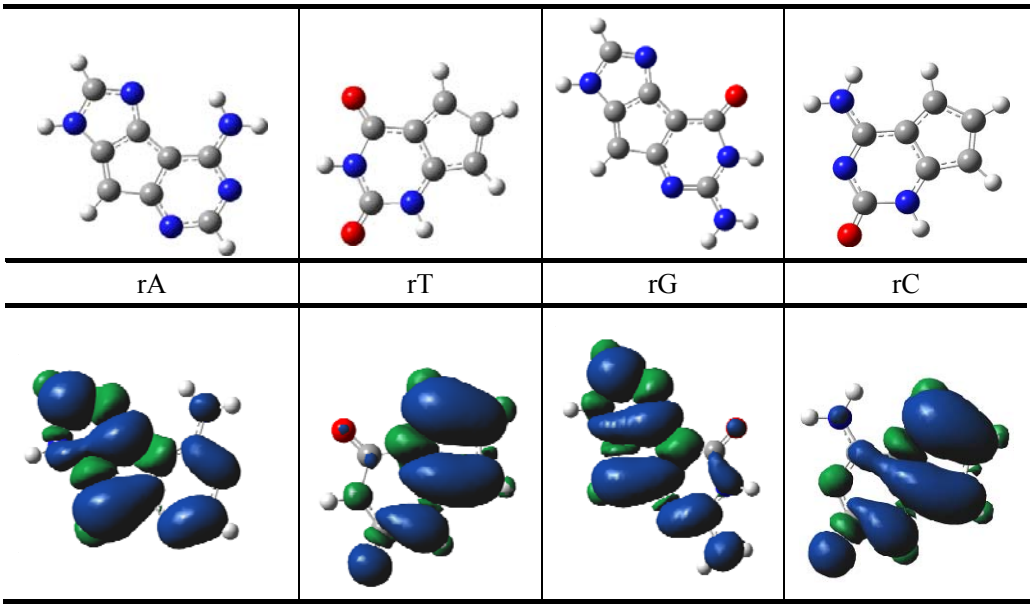

Figure S1. The spin densities distributions of optimized trans-r-bases

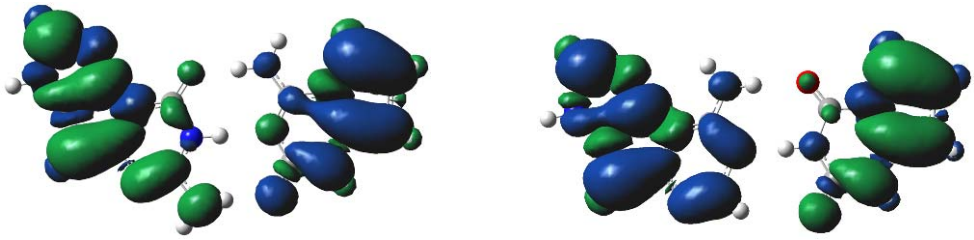

rG-rC rA-rT

Figure S2. The spin densities distributions of optimized trans-r-base pairs

Spin Densities Distributions in Overlap-Stacking Diradical Base Pairs.

rG-C/rG-C (BS)

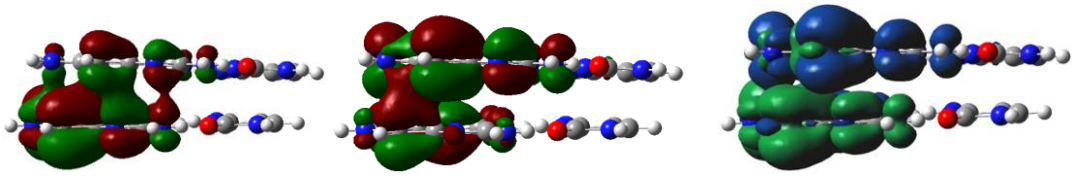

rG-C/rG-C (T)

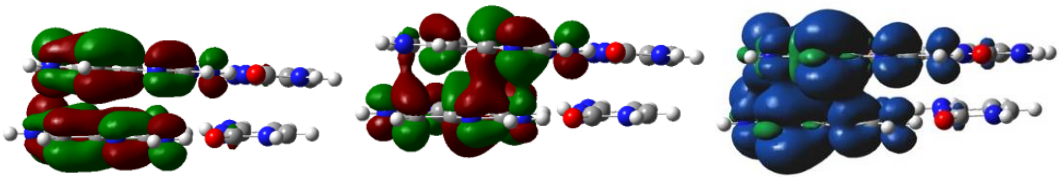

rG-C/rA-T (BS)

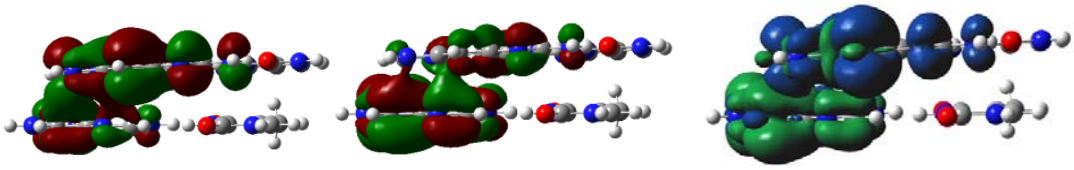

rG-C/rA-T (T)

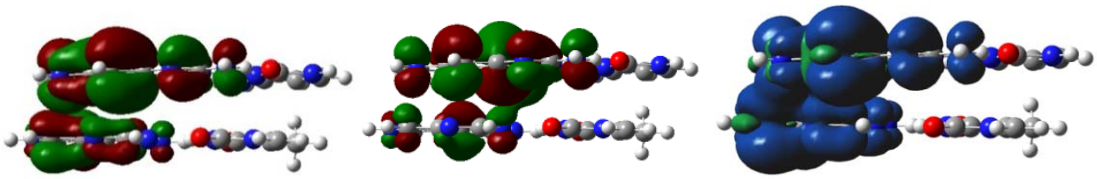

rA-T/rA-T (BS)

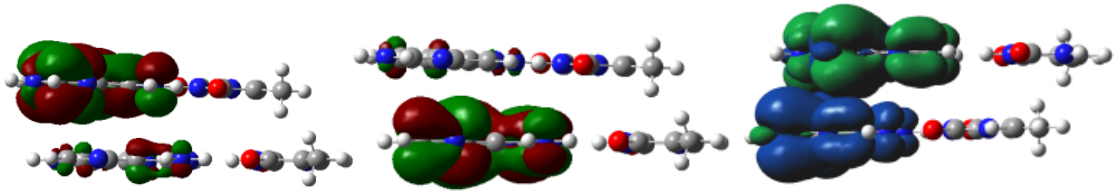

rA-T/ rA-T (T)

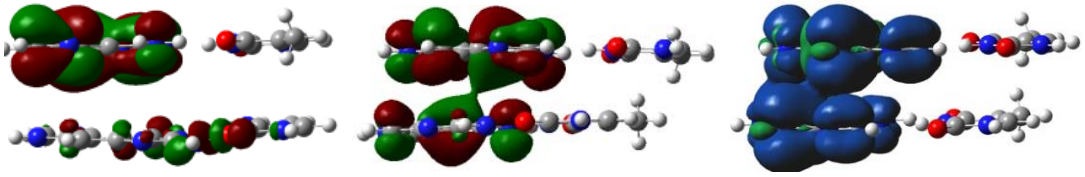

rA-T/rG-C (BS)

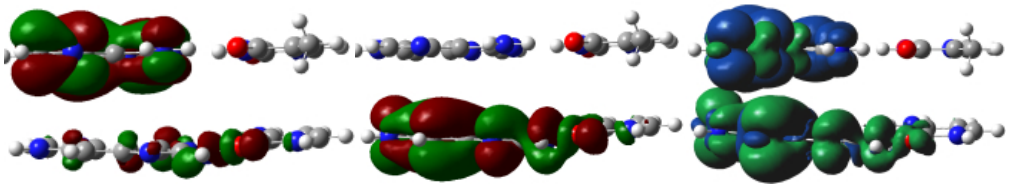

rA-T/rG-C (T)

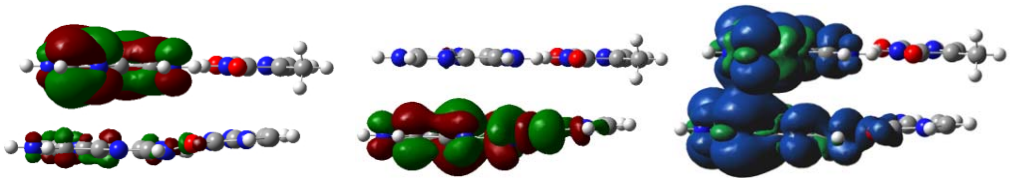

Figure S3. SOMOs / spin density maps for open-shell singlet states and open-shell triplet of the overlap-stacking trans-r-base pairs in 3'-r-purine/5'-r-purine model.

A-rT/A-rT (BS)

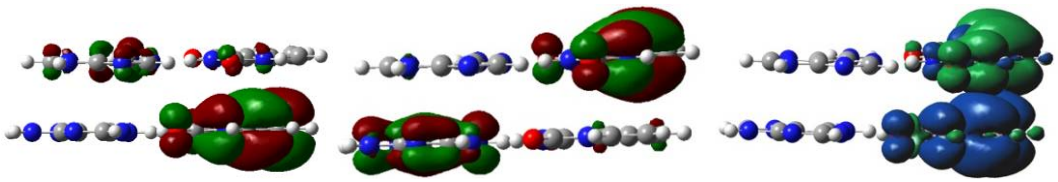

A-rT/G-rC (BS)

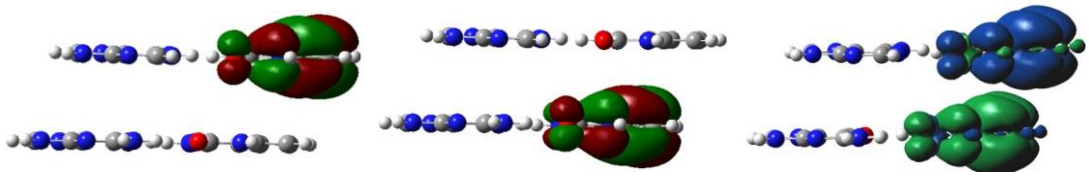

G-rC/G-rC(BS)

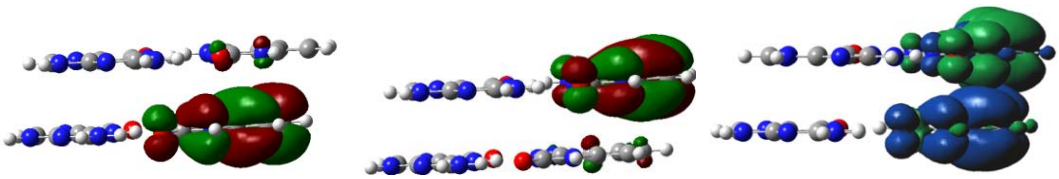

G-rC/A-rT(BS)

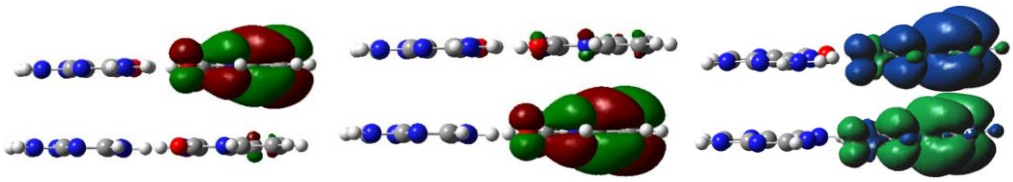

Figure S4. SOMOs / spin density maps for open-shell singlet states of the over-stacking trans-r-base pairs in 3'-r-pyrimidine/5'-r-pyrimidine model.

rG-C/rC-G (BS)

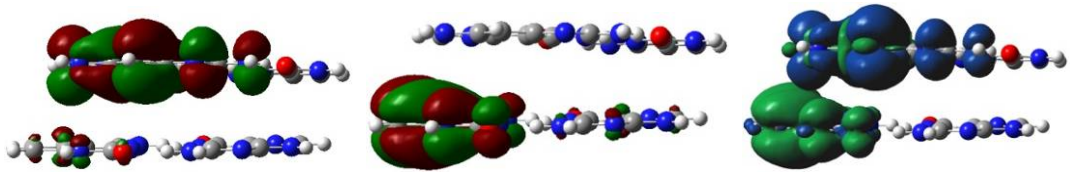

rG-C/rT-A (BS)

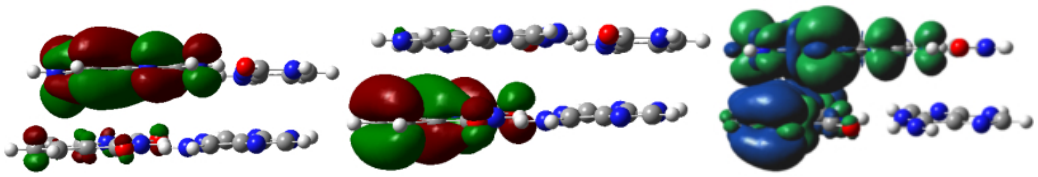

rA-T/rC-G (BS)

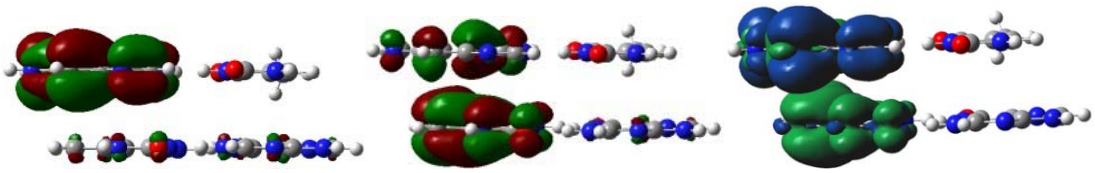

Figure S5. SOMOs / spin density maps for open-shell singlet states of the over-stacking trans-r-base pairs in 3'-r-purine-5'-r-pyrimidine model.

rC-G /rG-C (BS)

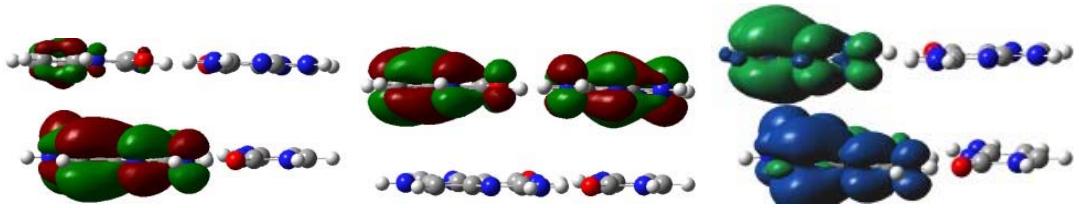

rC-G/rA-T (BS)

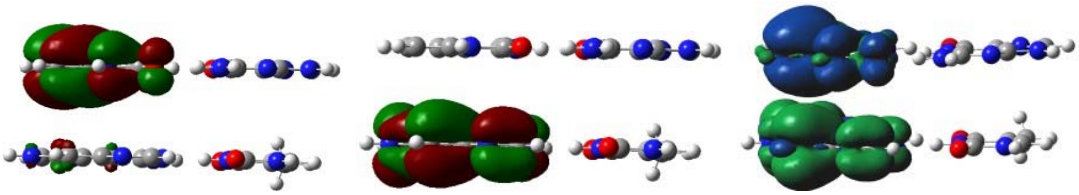

rT-A/ rA-T (BS)

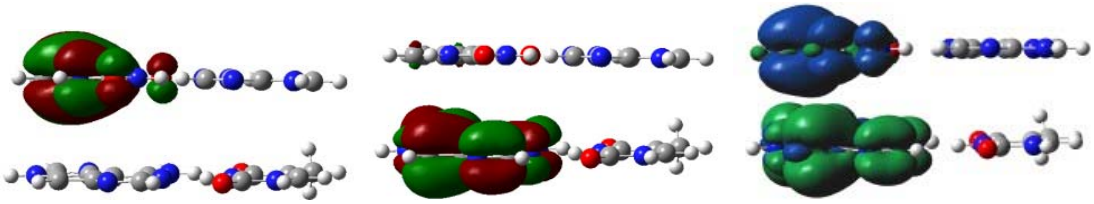

rT-A/rG-C(BS)

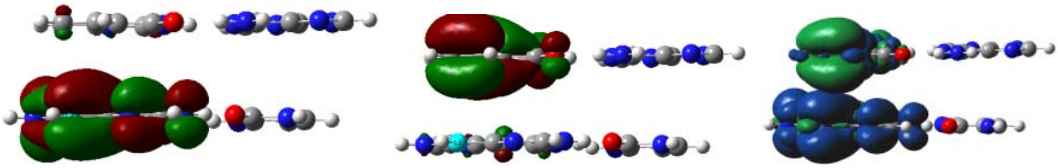

Figure S6. SOMOs / spin density maps for open-shell singlet states of the over-stacking trans-r-base pairs in 3'-r-pyrimidine-5'-r-purine model.

Spin Densities Distributions in Cross-Stacking Diradical Base Pairs.

rG-C/C-rG (BS)

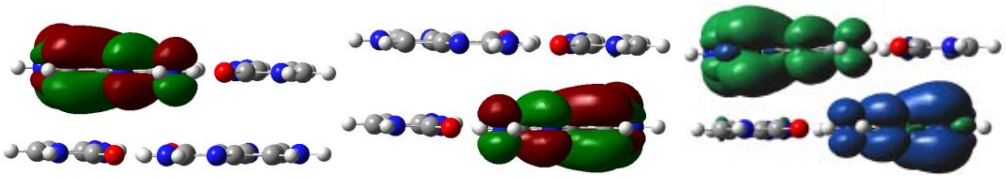

rG-C/T-rA (BS)

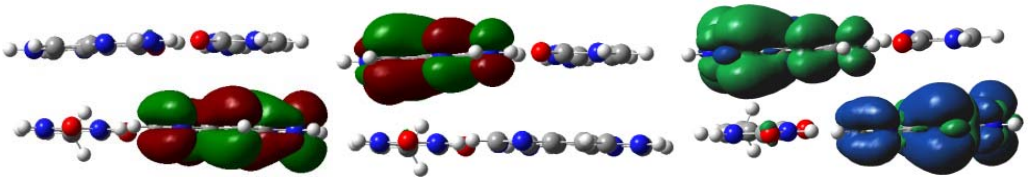

rA-T/T-rA (BS)

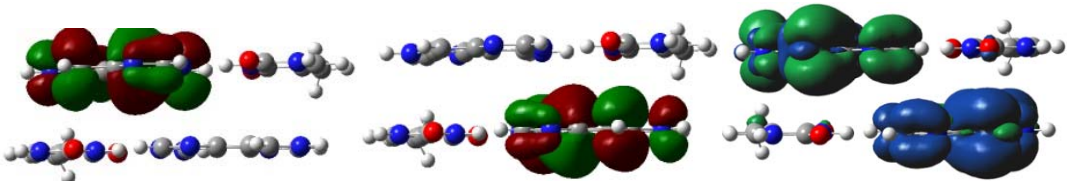

Figure S7. SOMOs / spin density maps for open-shell singlet states of the cross-stacking trans-r-base pairs in 3′-r-purine/3′-r-purine model.

G- rC /rC-G(BS)

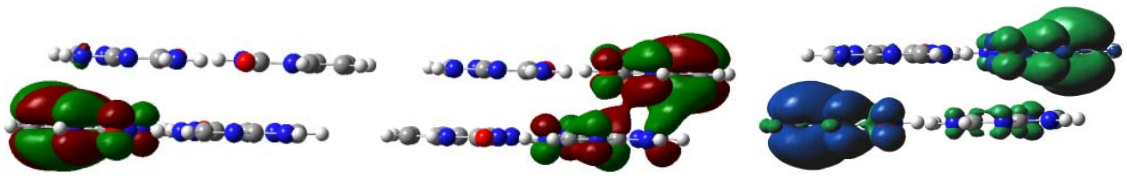

G-rC/rT-A(BS)

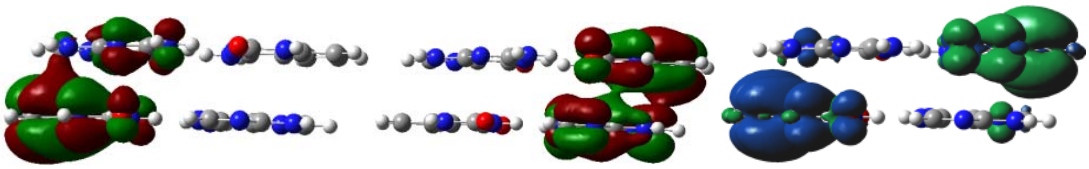

A-rT/rT-A(BS)

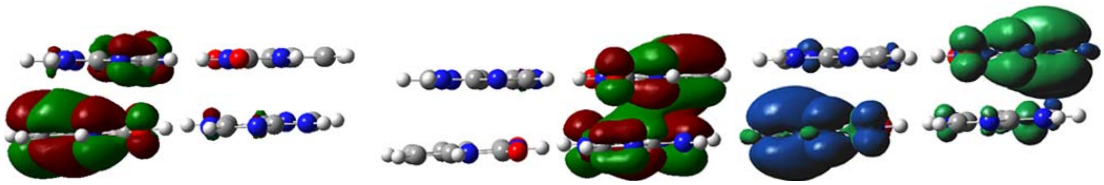

Figure S8. SOMOs / spin density maps for open-shell singlet states of the cross-stacking trans-r-base pairs in 5′-r-pyrimidine/5′-r-pyrimidine model.

rT-A /A-rT(BS)

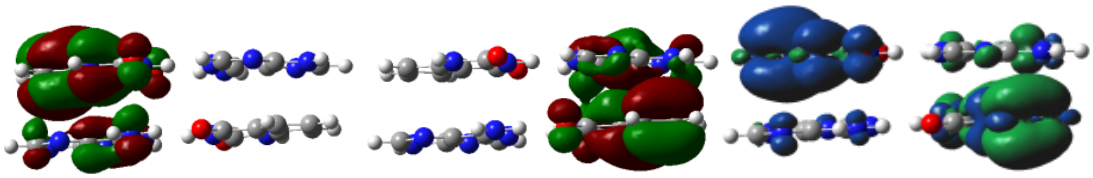

rC-G /A-rT(BS)

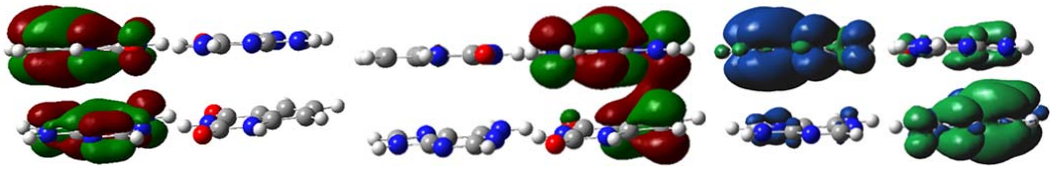

rC-G /G-rC(BS)

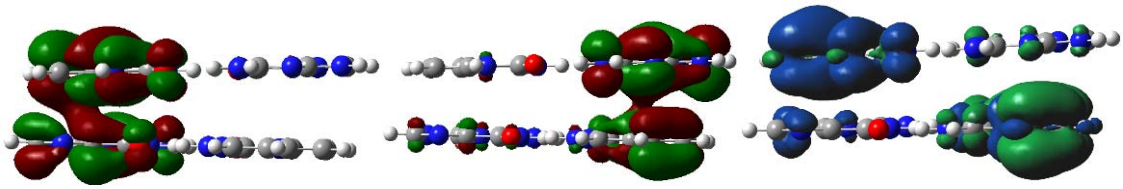

Figure S9. SOMOs / spin density maps for open-shell singlet states of the cross-stacking trans-r-base pairs in 3′-r-pyrimidine/3′-r-pyrimidine model.

rA-T/A-rT (BS)

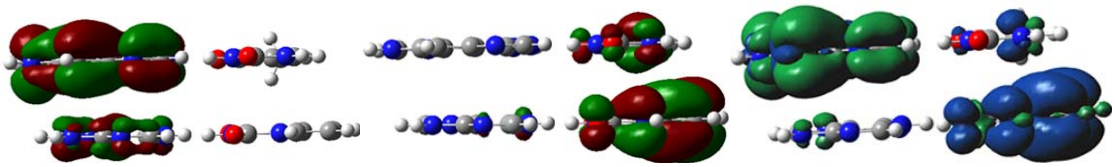

rA-T/G-rC (BS)

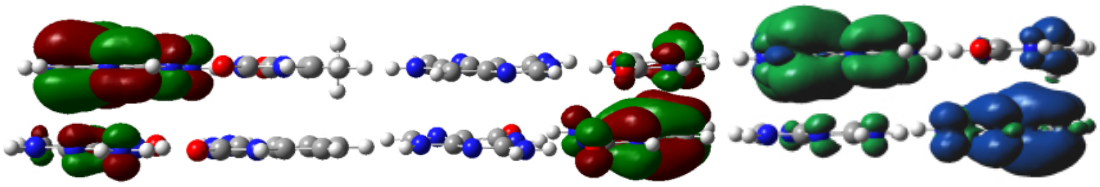

rG-C/A-rT (BS)

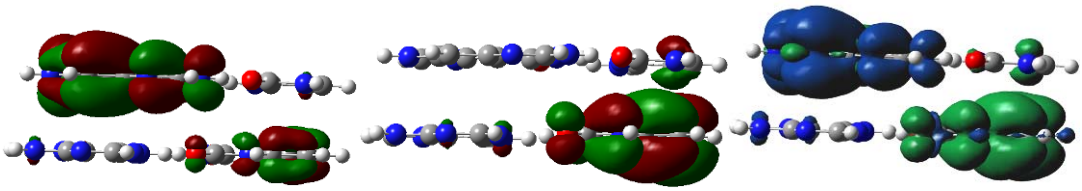

rG-C/G-rC (BS)

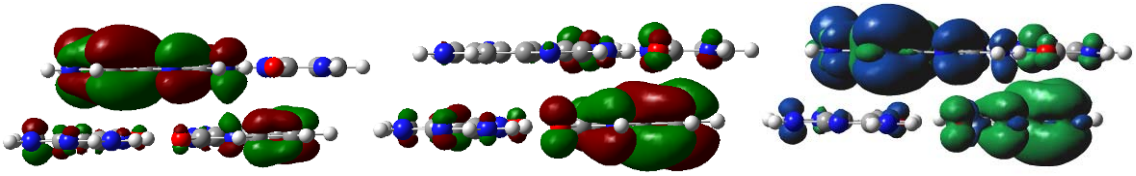

Figure S10. SOMOs / spin density maps for open-shell singlet states of the cross-stacking trans-r-base pairs in 3′-r-purine/3′-r-pyrimidine model.

A-rT/ rG-C (BS)

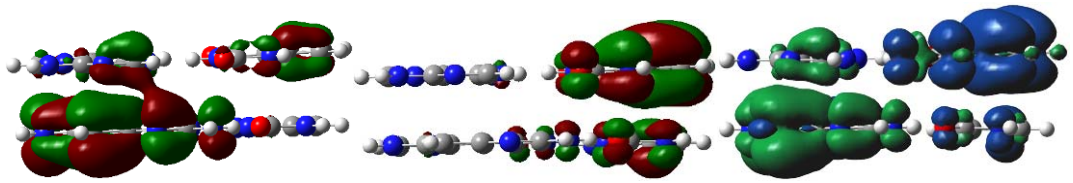

A-rT/ rA-T (BS)

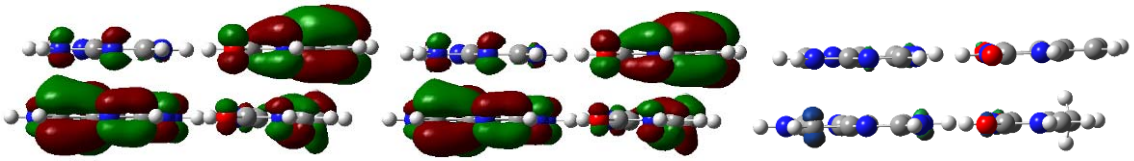

G-rC/ rG-C (BS)

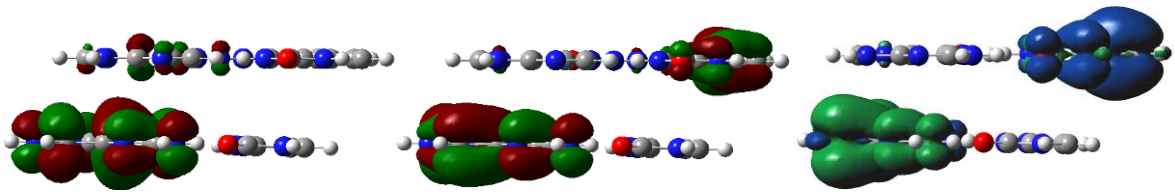

Figure S11. SOMOs / spin density maps for open-shell singlet states of the cross-stacking trans-r-base pairs in 5′-r-pyrimidine/5′-r-purine model.

C-rG/rG-C (BS)

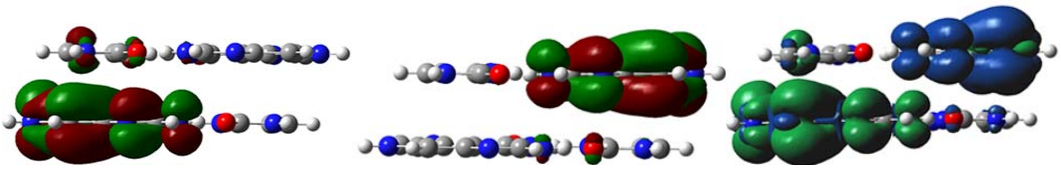

C-rG/rA-T (BS)

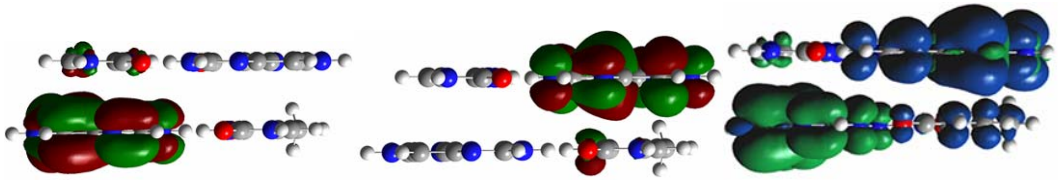

T-rA/rA-T (BS)

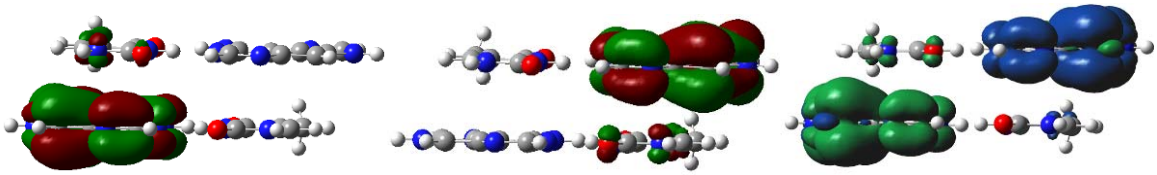

Figure S12. SOMOs / spin density maps for open-shell singlet states of the cross-stacking trans-r-base pairs in 5′-r-purine/5′-r-purine model.

rG-rC/ rG-rC (BS)

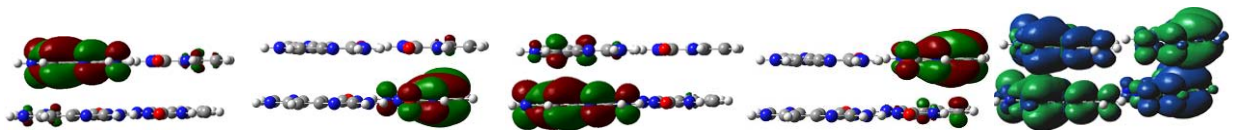

rC-rG/ rG-rC (BS)

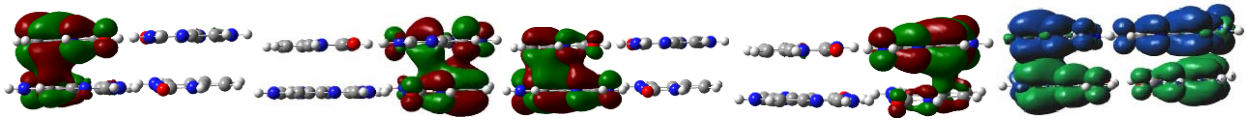

Figure S13. SOMOs / spin density maps for open-shell singlet states of tetra-radical trans-r-base pairs.

rG-rC/ rT-rA (BS)

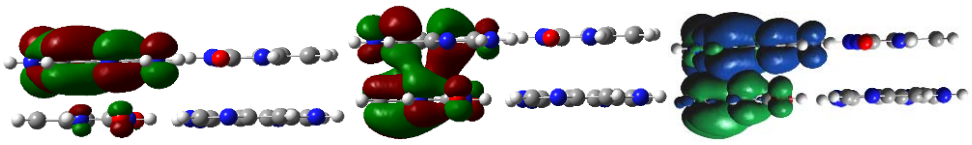

rA-rT/ rG-rC (BS)

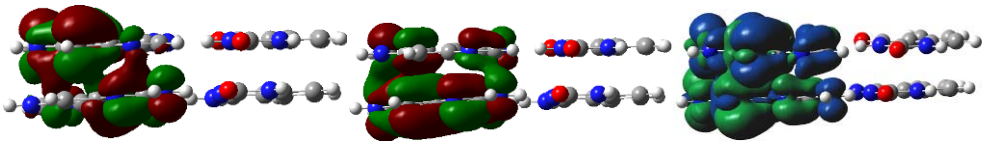

rC-rG/ rA-rT (BS)

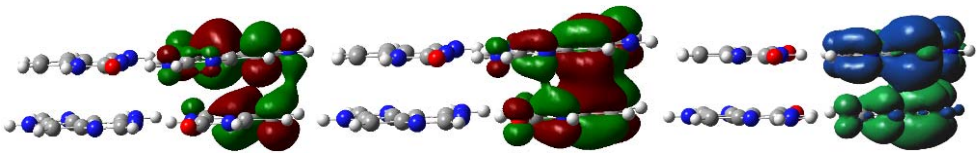

rT-rA/ rA-rT (BS)

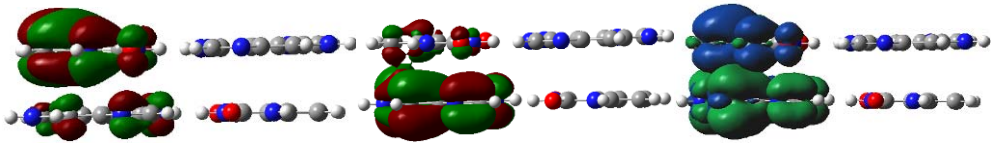

rG-rC/ rA-rT (BS)

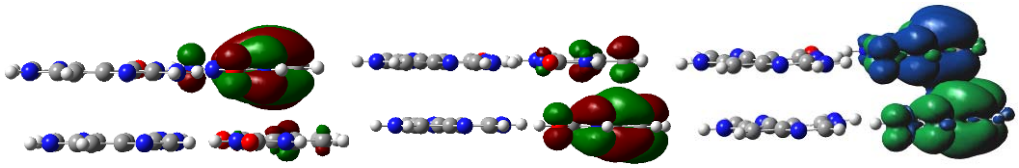

rG-rC /rC-rG (BS)

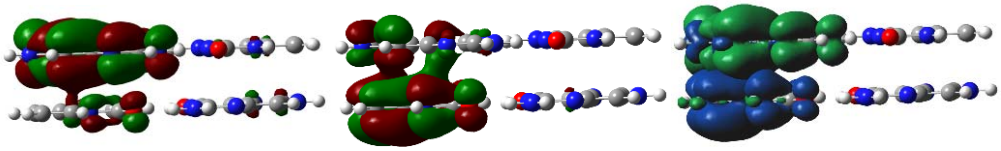

Figure S14. SOMOs / spin density maps for open-shell singlet states of diradical trans-r-base pairs.

BPs	UB3LYP/6-311++G**			UM062X/6-311++G**		
	SOMO- α	SOMO- β	Spin Density	SOMO- α	SOMO- β	Spin Density
rT-A/rA-T	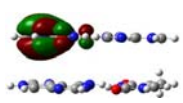	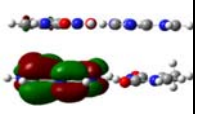	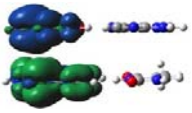	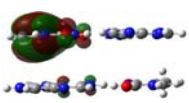	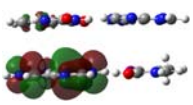	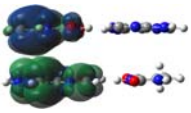
rT-A/rG-C	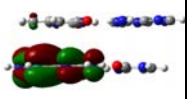	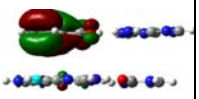	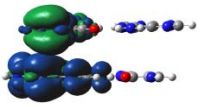	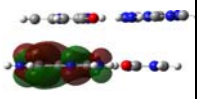	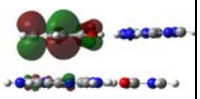	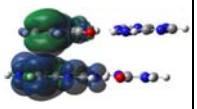
rC-G/G-rC	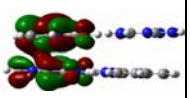	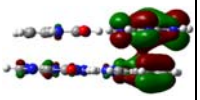	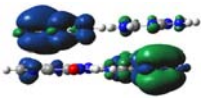	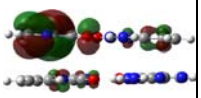	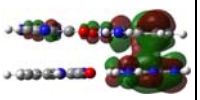	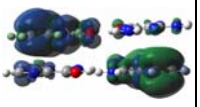
rA-T/T-rA	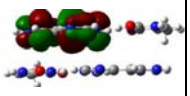	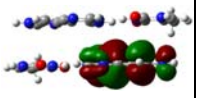	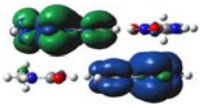	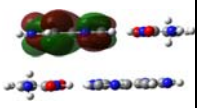	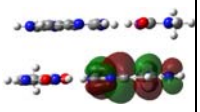	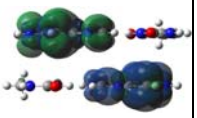
rC-G/rA-T	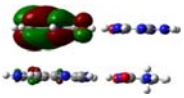	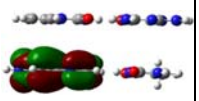	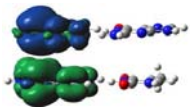	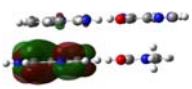	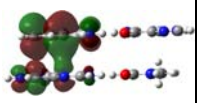	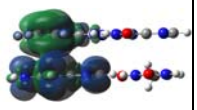
C-rG/rG-C	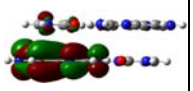	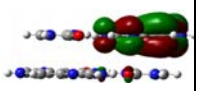	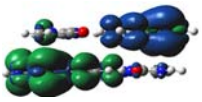	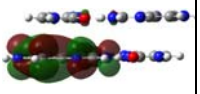	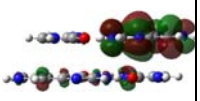	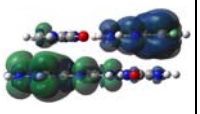
A-rT/G-rC	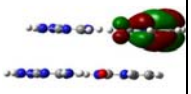	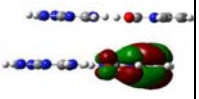	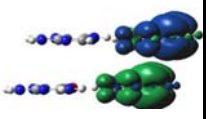	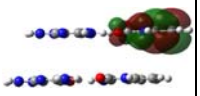		
T-rA/rA-T						

Figure S15. SOMOs / spin density maps for open-shell singlet states of part diradical trans-r-base pairs used with UB3LYP/6-311++G** and UM062X/6-311++G** Method.